ACS Photonics
Letter
pubs.acs.org/journal/apchd5

Salient Features of Deeply Subwavelength Guiding of Terahertz Radiation in Graphene-Coated Fibers

Artur R. Davoyan* and Nader Engheta*

Department of Electrical and Systems Engineering, University of Pennsylvania, Philadelphia, Pennsylvania 19104, United States

ABSTRACT: Here we discuss theoretically some of the notable features of modal characteristics in the graphene-coated deeply subwavelength fiber waveguide, providing a performance comparison between this guided-wave structure and some other typical THz waveguides. We highlight a cutoff-free propagation of a fundamental graphene-plasmon mode with an effective mode area, which can in principle be smaller than $(\lambda/100)^2$. We also discuss the phonon-plasmon hybridization that is expected for waveguides with polar dielectric core (e.g., SiO_2 and SiC). We believe that this guiding structure, being at the intersection of optics and electronics, may pave the way for a variety of nanoscience applications.

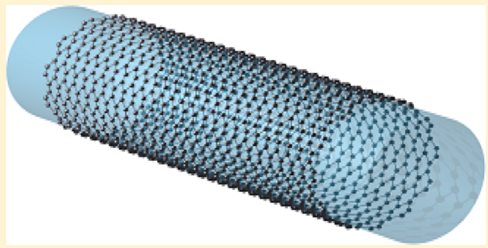

KEYWORDS: *graphene, fiber, subwavelength, plasmonics*

At the interface of conventional electronics on the one hand and photonics on the other, terahertz science is emerging as one of the major areas of research.[1,2] Various picosecond-scale processes and a diverse range of applications within this frequency band (0.1−10 THz) make the terahertz domain an attractive and rapidly growing field. Spectroscopy, imaging, sensing, ultrafast computing, information and telecommunications, biomedical research, and astrophysics are the few out of many areas to name, where terahertz technology is playing a central role.[1,2] Nonetheless, the lack of efficient sources and detectors of terahertz radiation (the problem of so-called "terahertz gap") poses significant limitations for further developments in this field.[1] These limitations, arising due to the nature of light/material interaction at terahertz frequencies, are imprinted also onto the design of terahertz systems for light control, manipulation, and, most importantly, radiation guidance. Of a major challenge is the design of efficient nanometer-scale-mode-area terahertz waveguides that may guide light confined well below the diffraction limit.[3−9] Such systems, if available, would quickly find their use in diverse fields of science and technology, varying from a high resolution nanometer THz imaging and spectroscopy to an on-chip bridging of photonics and electronics for ultrafast computing.[1−3] A nanometer-scale-mode-area terahertz guiding in graphene-coated fiber waveguides is an excellent candidate.[10−12] Here, we discuss some of the unique properties of two-dimensional materials, such as graphene, and we highlight some of the salient features of highly confined cutoff free terahertz guided modes in graphene-coated fibers. We also offer a comparison of performance (i.e., waveguide quality factor and modal confinement) between this guided-wave structure and some other available THz guiding systems, and theoretically demonstrate that the characteristics of such waveguides may be higher or comparable with those systems. The schematic of our comparison is shown in Figure 1 (see Methods for some specific points about this comparison.) We also discuss some aspects of phonon-plasmon hybridization that is expected in waveguides with polar dielectric cores (e.g., SiO_2 and SiC).

Interaction of light with metals and dielectrics that serve as building blocks for microwave and optical systems, at terahertz frequencies is accompanied by an enhanced absorption. This together with a relatively large free-space wavelength of THz radiation (∼300 μm) constrains miniaturization and on-chip integration of THz systems[3]. The interplay of these two factors, namely attenuation and confinement, leads to a trade-off in the design of terahertz waveguides and systems that rely on such waveguides.[13] In Figure 1 we symbolically show and qualitatively compare the performance (waveguide quality factor and confinement) of several of commonly used waveguides and trace conceptually the trend of their properties with frequency, from microwaves to optics. Metal-based waveguides dominate the radio and microwave frequency bands; these constitute the core of microwave and radio frequency (RF) metamaterial engineering.[14,15] Low losses (since metals essentially behave approximately as perfect electric conductors (PEC)) together with the ability for subwavelength radiation confinement between two conductors (e.g., in a coaxial waveguide, in a microstrip transmission line, or in a twin wire) allow designing metal-based waveguides with desired transmission and confinement characteristics.[14,15] At near-infrared and optical wavelengths, low-loss dielectric waveguides, such as fibers, are widely used for signal transmission.[13,16,17] These systems, however, cannot squeeze radiation well beyond the light diffraction limit, which is typically of the order of the wavelength. However, light may be coupled with electron density waves in metals with an excitation of highly localized surface plasmon-polaritons at optical frequencies.[18] This offers a reliable, thought quite lossy,

Received: September 7, 2015
Published: April 15, 2016

DOI: 10.1021/acsphotonics.5b00503
ACS Photonics 2016, 3, 737−742

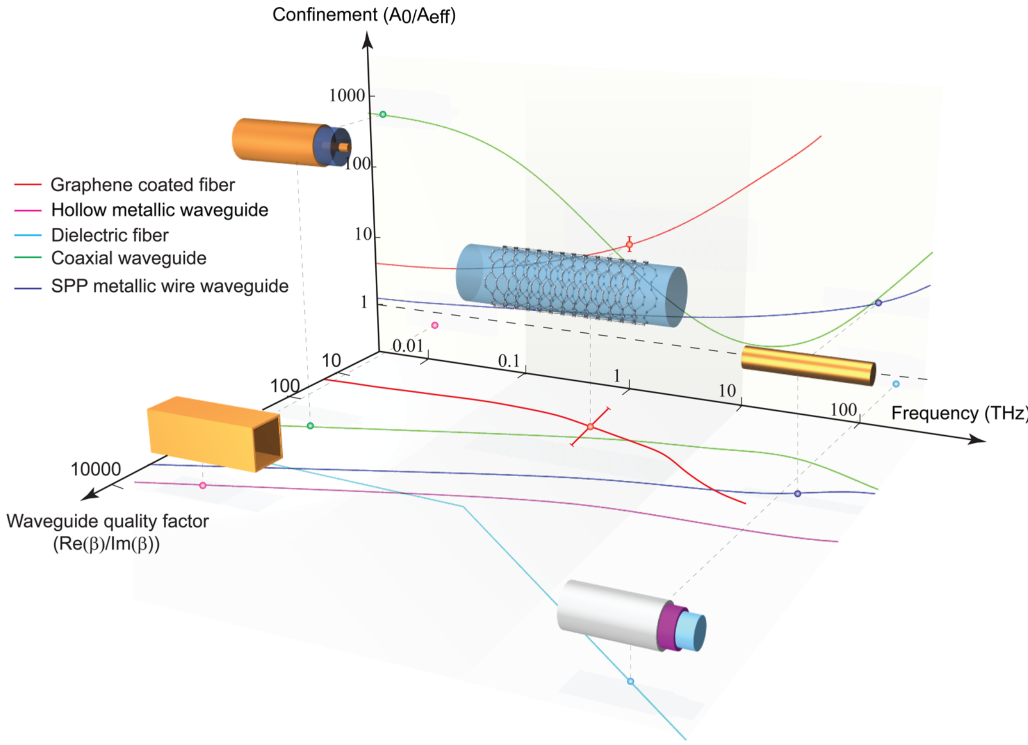

Figure 1. Performance map for conventional waveguides and the graphene-coated fiber waveguide ("meta-tube"). Plots of confinement (inverse of the normalized effective mode area) and waveguide quality factor (Re(beta)/Im(beta), proportional to inverse of attenuation) vs frequency are shown. Here, for all the frequency range we assume that the fiber and the hollow metallic waveguide have cross-section (radius) of the order of $r = \lambda$ (corresponding confinement curves are not present here, see Methods for details). For a wire, coaxial cable, and a graphene-coated fiber, we assume the radius $r = \lambda/50$. Metal is modeled based on the Drude model for copper. For graphene we use conductivity model and parameters according to recent experiment.[25] We assume Fermi energy, $E_f = 0.2$ eV, Fermi velocity, $v_f = 10^6$m/s, and electron relaxation time, $\tau = 1.6 \times 10^{-12}$s. The "error bars" denote the performance boundaries for a graphene-coated fiber for two different limiting values of electron relaxation time (i.e., different electron mobilities): $\tau \simeq 10^{-13}$ s and 10^{-11} s. For more details regarding material parameters, see Methods.

mechanism for subwavelength light guidance and steering at visible and near-infrared frequencies.[19] Again, with proper combination of metals and dielectrics and suitable structural design, optical waveguides with desired transmission characteristics, that is, desired balance between attenuation and confinement may be crafted.[20]

The situation is quite different for the terahertz frequency band in which metals neither behave as perfect electric conductors, nor support highly localized plasmons (the example of a subwavelength metallic wire ($\sim\lambda/50$ radius) shows that surface waves become weakly confined at terahertz and microwave frequencies, see Figure 1). Subwavelength guiding by two conductors (e.g., in a coaxial waveguide) implies rather strong wave attenuation; the attenuation is even higher for stronger wave confinement (thus for a $\sim\lambda/50$-radius coaxial waveguide the propagation distance hardy reaches 100 guided wavelengths at 1 THz, even in the case of almost lossless dielectric cladding, as well as confinement drops significantly). It is worth mentioning here recent breakthroughs with THz metamaterial structures in which rather efficient subwavelength guiding of terahertz radiation confined to dimensions of around $\sim\lambda/10$ (i.e., 30 μm at 1 THz) is possible.[6,8,9] However, the design of a truly nanometer size terahertz waveguides (~10–100 nm) indeed remains a challenge.

Two-dimensional materials such as graphene and boron nitride that exhibit unique electronic and photonic properties may be the key toward creating efficient THz systems and waveguides.[21−32] Importantly, in these systems highly localized electromagnetic excitations such as plasmon-polaritons[24−30] and phonon-polaritons[31,32] may be excited. Several planar geometries have been proposed earlier in the context of deeply subwavelength terahertz waveguides.[29,30] Here we discuss some of the important guiding features of a conceptually different guiding system, that is, a graphene-plasmon based waveguide that may be merged with current fiber and coaxial waveguiding technologies. We note that waveguides with a similar cylindrical topology have been reported in some recent works;[10−12] however, comprehensive analysis of light confinement and attenuation with frequency of operation and waveguide radius, study of the core induced phonon-plasmon hybridization, and comparison with other typical THz waveguides is missing in the earlier work. Here, we discuss these additional features, in addition to underlining the fundamental difference between cutoff free modes found in such graphene-coated fiber and the edge states in graphene nanoribbon waveguides.[29,30]

In a regular dielectric fiber light guiding is achieved in the high index core.[16] Depending on the radius of the system and the operating frequency, different modes may be excited.[16] Figure 2A shows the dispersion of several of lower order fiber modes for a 5 μm radius fiber waveguide with dispersionless core relative permittivity of 2.5 (similar to that of SiO_2 in a rather large frequency span[25] or that of a low loss polymers, such as polystyrene and polyethylene,[33−35] frequently used in microwave waveguide technology). Below 700 cm^{-1} (21 THz), the fiber operates in a single-mode regime; only fundamental hybrid electric mode (HE_{11}) is supported. This mode does not have cutoff and, in principle, may be excited for arbitrarily small waveguide radius or operating frequency.[17] However, below a

DOI: 10.1021/acsphotonics.5b00503
ACS Photonics 2016, 3, 737−742

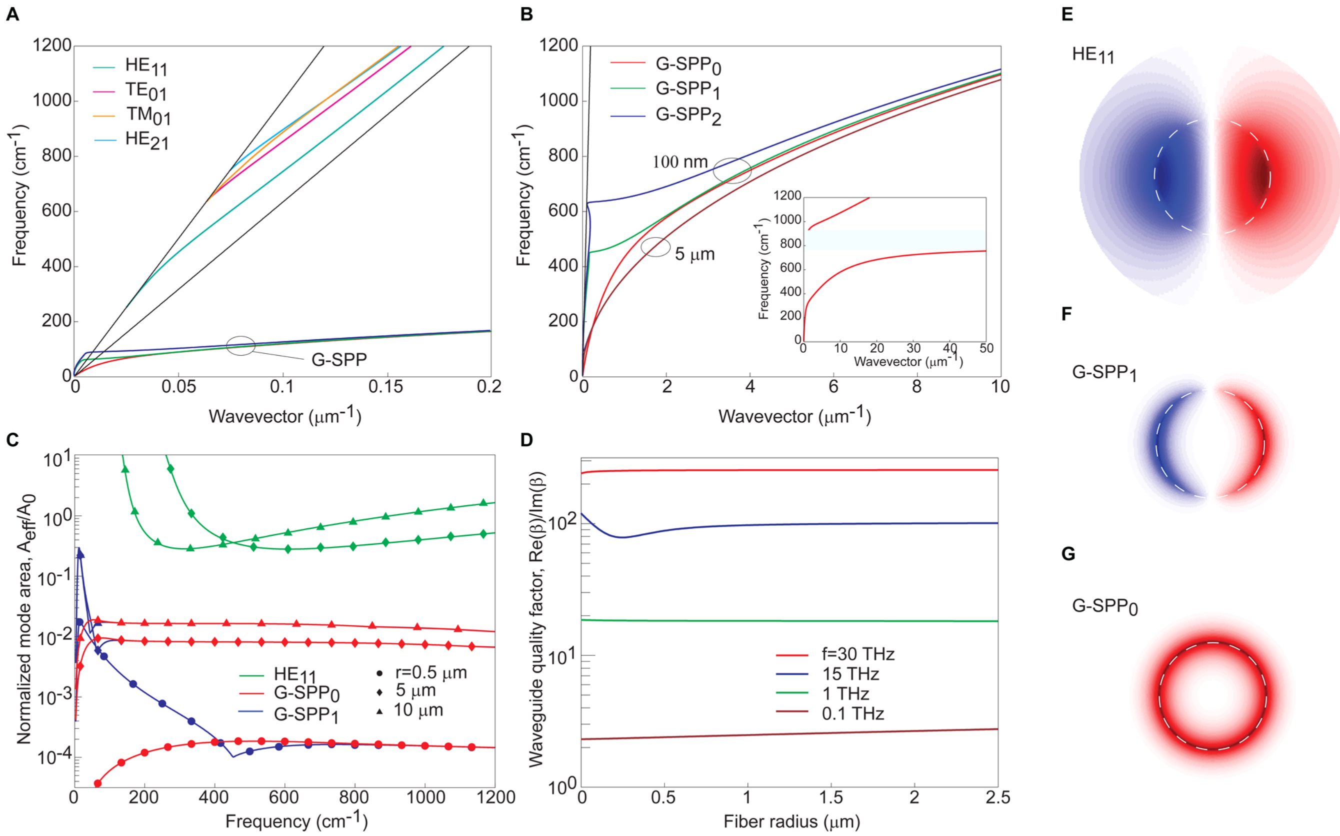

Figure 2. Modal properties of a graphene-coated fiber. (A) Dispersion of fiber modes in a 5 μm fiber. (B) Dispersion of graphene plasmon modes only for 100 nm and 5 μm fibers, respectively. Solid black lines in (A) and (B) correspond to light lines. Inset shows the dispersion of a 100 nm SiC graphene-coated fiber. The properties of SiC are taken from ref 26. Shaded region denotes the range of frequencies where SiC has a negative permittivity. (C) Confinement of HE_{11} and graphene-plasmon modes for several fiber waveguides with different radii. (D) Inverse of attenuation of fundamental graphene plamson modes with fiber radius for several characteristic frequencies. (E−G) Typical snapshots mode profiles of the guided fiber and graphene-plasmon modes. Blue color corresponds to the field minimum and red to the field maximum, respectively.

certain critical frequency its transverse confinement drops significantly and the HE_{11} mode extends into the surrounding medium[17] (for the waveguide considered here this frequency is around 300 cm^{-1} (9 THz)), see Figure 2C,E. Hence, confined light guiding with the use of regular fiber modes is challenged for frequencies below 10 THz. Coating the fiber with graphene (such a technology was previously utilized for the design of electro-optical modulators[36−38]), it is possible to excite modes of a new kind, graphene plasmon-polariton modes.[24−30] These modes may have guide indices up to 2 orders of magnitude higher than the refractive index of the core, see Figures 2A.

Figure 2B shows the dispersion of the several of lower order graphene plasmon-polariton modes (denoted as G-SPP) for 5 μm and 100 nm radius fiber waveguides, respectively. For electrically large waveguide radius (i.e., for $R \geq \lambda$, where λ is the free-space wavelength and R is the waveguide radius) the dispersion of the graphene-plasmon fiber modes resembles that of plasmon-polaritons in a single layer of graphene.[27,28] This degeneracy is removed at lower frequencies (i.e., for $\lambda \gg R$), see Figure 2A,B. Interestingly, the fundamental azimuthally symmetric mode (G-SPP0) does not have cutoff frequency and may, in principle, be confined and guided in waveguides with arbitrarily small radius, in contrast to a regular HE_{11} mode. It is this dynamics that makes this mode a promising candidate for a nanometer-scale-diameter terahertz light guiding and focusing. Plasmon propagation in carbon nanotubes may be viewed as a limiting scenario of this case.[39,40] We note that cutoff-free propagation has been also reported in graphene nanoribbons for the case of edge plasmon modes.[29,30] However, the G-SPP0 mode of the fiber waveguide shown in Figure 2 and the plasmonic edge state predicted for the graphene nanoribbon are not topologically equivalent, implying fundamentally different field profiles, dispersions, as well as excitation regimes (ref 30 underlines this fundamental difference for a planar graphene film). Moreover, the nanoribbon plasmons, featuring the dispersion of unbounded graphene plasmons (i.e., ribbon modes that are not bound to graphene edges), exhibit a distinct half-wavelength cutoff.[30] Edge plasmon states despite revealing an exciting physics due to their inherently reduced, "point-like" dimensionality (as compared with "regular" two-dimensional plasmons) are hardly compatible with integrated optics platforms, limiting their potential use. In contrast, the system discussed here offers a natural bridge between conventional photonics and deeply subwavelength graphene plasmonics.

It is also noteworthy to compare the G-SPP modes with plasmons in metallic nanowires.[41−43] In principle, one might think of a graphene fiber as a limiting scenario of a hollow core metallic nanowire with infinitesimally thin walls.[42,43] However, these two systems exhibit conceptually different light guiding mechanisms. Plasmon modes in metal-dielectric systems originate due to hybridization between the free propagating radiation and bulk plasma waves, which leads to a distinct surface plasmon-polariton resonance.[18] The fundamental plasmonic mode in such systems is strongly localized near

DOI: 10.1021/acsphotonics.5b00503
ACS Photonics 2016, 3, 737−742

this resonance, however the localization steeply decreases as the plasmon dispersion reaches the light-line with as the frequency decreases,[18,41−43] see also Figure 1. In graphene and other two-dimensional electron gases the plasmon dispersion has a fundamentally different nature.[27,28] Within the frame of Drude model the dispersion of 2D plasma waves of an unbounded graphene film is, in principle, free of resonances and follows a square root dispersion law.[27,28] This behavior is of a significant interest as the modes can be strongly confined to a graphene interface within a large bandwidth. The fundamental G-SPP mode of the graphene fiber waveguide inherits this behavior (see Figure 2b), making graphene-coated fiber a promising candidate for the deep subwavelength radiation guiding.

To study confinement of graphene-plasmon and regular HE_{11} fiber modes, we plot the normalized mode cross-sectional area,[44] which is defined as $\frac{A_{eff}}{A_0} = ([\int Ida]^2/\int I^2da)\frac{1}{(\lambda^2/4)}$ (here A_{eff} is the effective mode area, $A_0 = \lambda^2/4$ is an equivalent of a mode area of a diffraction limited spot, and I is the intensity distribution in the waveguide) in Figure 2C. Both G-SPP_0 and G-SPP_1 modes are highly localized in comparison with the HE_{11} fiber mode. Typical snapshots of field profiles of the modes of interest are shown in Figure 2E−G. The confinement of graphene-plasmon fiber modes increases even further as the radius decreases. Thus, for a 500 nm radius waveguide the graphene-plasmon modes occupy an area less than 0.0001 λ^2; that is, for a free space wavelength of $\lambda \simeq 300$ μm, the effective radius of the G-SPP_0 mode is <1 μm. Beyond a certain critical frequency higher order graphene modes lose their confinement and localization, which corresponds to an effective cutoff for these modes (see Figure 2C, as well as Figure 2A,B). Similar dynamics is observed for HE_{11} fiber modes, as mentioned earlier. Note also that above the cutoff higher order G-SPP modes being of multipolar origin are more confined to the graphene interface as compared to the fundamental monopolar G-SPP0 mode.

In Figure 2D, the normalized waveguide quality factor (i.e., $\frac{Re(\beta)}{Im(\beta)} = \frac{L}{2\lambda_g}$, where L is the propagation distance, λ_g is the guided wavelength, β is the guide index) is shown for the G-SPP_0 graphene plasmon modes. Interestingly, the mode attenuation does not depend as much on the fiber radius, as it depends on the frequency of operation. As expected, the attenuation is lower for higher operating frequencies (which correlates well with plasmons in a single interface graphene[27,28]). For example, for the graphene parameters we use, it reaches 10−15 plasmon wavelengths at around 1THz and ~100 plasmon wavelengths at around 10−15 THz. High confinement and relatively low attenuation of the G-SPP0 mode make such a graphene-coated fiber an interesting candidate for efficient nanometer scale light guiding. We compare the performance of the graphene-coated fiber with some other commonly used waveguides in Figure 1, clearly in a range of frequencies 1−10 THz, the graphene-coated fiber may compete with the performance of coaxial and similar microwave inspired waveguides, even for moderate values of electron relaxation times[30] ($\tau = 1.6 \times 10^{-12}$ s).

Finally, we note that the dispersion of plasmons in graphene is strongly affected by the substrate on which graphene is deposited.[25,26] For instance, silicon carbide, typically used as a substrate for graphene, exhibits a polaritonic resonance around 800 cm^{-1}, implying graphene-plasmon SiC-polariton hybridization[26] (similar effects have been reported also for boron nitride[45] and SiO_2,[25] and the analysis below is applicable to these cases, too). To illustrate that this graphene-coated fiber concept is working in this case as well we plot the dispersion of the fundamental G-SPP mode for a graphene-coated SiC fiber in the inset to Figure 2B. In this case, hybridization of graphene-plasmon fiber mode with the SiC polariton is observed in our calculation, as expected[26] (a similar effect is anticipated for the SiO_2, another typical graphene substrate,[25] at around 30 THz as well). Interestingly, the guide indices in this case are an order of a magnitude higher than that for a graphene coated fiber with a regular dielectric core (as studied above); this implies even stronger mode confinement at the graphene interface. Away from a rather narrow polaritonic resonance in SiC,[26] the dissipation in SiC core plays a minor role. We also note that purely polaritonic systems are also of interest,[31,32] and the ideas discussed here may be extended to other classes of two-dimensional materials,[22,23] such as boron-nitride.[32]

The graphene-coated fiber waveguide discussed here offers an exciting platform for a nanometer-size terahertz technology. Not only may this system be utilized for deep subwavelength waveguiding that is important for imaging and nanoscale spectroscopy, but also it may open new opportunities for merging electronics and photonics on a simple naturally integrated platform: High-speed interconnects; THz modulators; THz nanolasers and detectors; optoelectronic mixers are just a few out of a large number of possible applications that one may envision.

■ METHODS

The analysis of the mode propagation in graphene coated fiber waveguide and other cylindrical structures shown in Figure 1 is based on the study of a corresponding dispersion equations. The dispersion equation for the case of a graphene coated fiber is derived in a close analogy with that of a regular optical fiber[16,46] by imposing appropriate boundary conditions at the graphene interface ($\overline{n}_{12} \times (\overline{H}_2 - \overline{H}_1) = \sigma\overline{E}_{\parallel}$, where σ is the graphene conductivity, $\overline{n}_{12}$ is the unit vector normal to the fiber interface, $\overline{H}_{1,2}$ is the magnetic field vector inside and outside the fiber respectively, and $\overline{E}_{\parallel}$ is the tangential (i.e., continuous) component of the electric field at the graphene interface).

The dielectric core in the coaxial waveguide in Figure 1 is chosen to have a refractive index of 1.58 + 0.0003i corresponding to the permittivity of ultralow loss polymers.[33−35] This value of the refractive index is also correlated with that of the graphene coated fiber core (Figure 2), simplifying the comparison. The waveguide quality factor for regular fiber waveguides shown in the Figure 1 represents an upper bound of the performance deduced based on low-loss dielectric materials available for three characteristic frequency domains: microwave (~1 GHz), THZ (~1 THz), and infrared (i.e., the curve related to the fiber waveguide quality factor in Figure 1 is essentially an interpolation by three points). Thus, for the microwave and terahertz domains, we use a refractive index of 1.58 + 0.0003i corresponding to that of low-loss polymers (e.g., polystyrene and polyethylene[33−35]), as mentioned earlier. To estimate the upper bound of the propagation distances in fibers at infrared/visible we consider a ZBLAN dielectric with an index of refraction of 1.5 + $10^{-7}i$ (see ref 47).

We note also that the confinement curves for the hollow core metallic waveguide and a fiber waveguide is not plotted in Figure 1 for the sake of keeping the clarity of Figure 1. The

DOI: 10.1021/acsphotonics.5b00503
ACS Photonics 2016, 3, 737−742

confinement for these two waveguides is symbolically shown to be above the diffraction limit (i.e., less than unity in the vertical axis in Figure 1). The actual confinement for these two systems is bound by the geometry and the choice of the dielectric core. It is possible to get a subdiffraction light propagation in a high index dielectric waveguide; the light confinement in such systems is well-known and follows closely the dynamics shown in Figure 2C. Similarly, the size of the hollow core rectangular waveguide may be reduced by the use of high index core.[14] Finally, at visible frequency in a hollow core waveguide, highly confined surface plasmons may be excited;[41−43] in this case, the waveguide may be designed to be deeply subwavelength.

AUTHOR INFORMATION

Corresponding Authors

*E-mail: davoyan@seas.upenn.edu.

*E-mail: engheta@ee.upenn.edu.

Notes

The authors declare no competing financial interest.

ACKNOWLEDGMENTS

This work is supported in part by the U.S. Air Force Office of Scientific Research (AFOSR) Grant No. FA9550-10-1-0408.

REFERENCES

(1) Tonouchi, M. Cutting-Edge Terahertz Technology. *Nat. Photonics* **2007**, *1*, 97.

(2) Zhang, X.-C.; Xu, J. *Introduction to THz Wave Photonics*; Springer-Verlag: New York, 2009.

(3) Adam, A. J. L. Review of Near-Field Terahertz Measurement Methods and Their Applications. *J. Infrared, Millimeter, Terahertz Waves* **2011**, *32*, 976.

(4) Seo, M. A.; Park, H. R.; Koo, S. M.; Park, D. J.; Kang, J. H.; Suwal, O. K.; Choi, S. S.; Planken, P. C. M.; Park, G. S.; Park, N. K.; Park, Q. H.; Kim, D. S. Terahertz Field Enhancement by a Metallic Nano Slit Operating Beyond the Skin-Depth Limit. *Nat. Photonics* **2009**, *3*, 152.

(5) Schnell, M.; Alonso-Gonzalez, P.; Arzubiaga, L.; Casanova, F.; Hueso, L. E.; Chuvilin, A.; Hillebrand, R. Nanofocusing of Mid-Infrared Energy with Tapered Transmission Lines. *Nat. Photonics* **2011**, *5*, 283.

(6) Pendry, J. B.; Martın-Moreno, L.; Garcia-Vidal, F. J. Mimicking Surface Plasmons with Structured Surfaces. *Science* **2004**, *305*, 847.

(7) Rusina, A.; Durach, M.; Nelson, K. A.; Stockman, M. I. Nanoconcentration of Terahertz Radiation in Plasmonic Waveguides. *Opt. Express* **2008**, *16*, 18576.

(8) Maier, S. A.; Andrews, S. R.; Martín-Moreno, L.; García-Vidal, F. J. Terahertz Surface Plasmon-Polariton Propagation and Focusing on Periodically Corrugated Metal Wires. *Phys. Rev. Lett.* **2006**, *97*, 176805.

(9) Ishikawa, A.; Zhang, S.; Genov, D. A.; Bartal, G.; Zhang, X. Deep Subwavelength Terahertz Waveguides Using Gap Magnetic Plasmon. *Phys. Rev. Lett.* **2009**, *102*, 043904.

(10) Correas-Serrano, D.; Gomez-Diaz, J. S.; Alu, A.; Alvarez-Melcon, A. Electrically and Magnetically Biased Graphene-Based Cylindrical Waveguides: Analysis and Applications. *IEEE Trans. Terahertz Sci. Technol.* **2015**, *5*, 951.

(11) Gao, Y.; Ren, G.; Zhu, B.; Liu, H.; Lian, Y.; Jian, S. Analytical Model for Plasmon Modes in Graphene-Coated Nanowire. *Opt. Express* **2014**, *22*, 24322.

(12) Liu, J. P.; Zhai, X.; Wang, L. L.; Li, H. J.; Xie, F.; Lin, Q.; Xia, S. X. Analysis of Mid-Infrared Surface Plasmon Modes in a Graphene-Based Cylindrical Hybrid Waveguide. *Plasmonics* **2015**, 1−9.

(13) Atakaramians, S.; Afshar, S. V.; Monro, T. M.; Abbott, D. Terahertz Dielectric Waveguides. *Adv. Opt. Photonics* **2013**, *5*, 169−215.

(14) Balanis, C. A. *Advanced Engineering Electromagnetics*; Wiley, 1989.

(15) Engheta, N.; Ziolkowski, R. W. *Metamaterials: Physics and Engineering Explorations*; Wiley, 2006.

(16) Kumar, S.; Deen, M. J. *Fiber Optic Communications: Fundamentals and Applications*; Wiley, 2014.

(17) Brambilla, G. Optical Fibre Nanowires and Microwires: A Review. *J. Opt.* **2010**, *12*, 043001.

(18) Maier, S. A. *Plasmonics: Fundamentals and Applications*; Springer, 2007.

(19) Barnes, W. L.; Dereux, A.; Ebbesen, T. W. Surface Plasmon Subwavelength Optics. *Nature* **2003**, *424*, 824−830.

(20) Oulton, R. F.; Sorger, V. J.; Genov, D. A.; Pile, D. F. P.; Zhang, X. A Hybrid Plasmonic Waveguide for Subwavelength Confinement and Long-Range Propagation. *Nat. Photonics* **2008**, *2*, 496−500.

(21) Bonaccorso, F.; Sun, Z.; Hasan, T.; Ferrari, A. C. Graphene Photonics and Optoelectronics. *Nat. Photonics* **2010**, *4*, 611−622.

(22) Britnell, L.; Ribeiro, R. M.; Eckmann, A.; Jalil, R.; Belle, B. D.; Mishchenko, A.; Kim, Y. J.; Gorbachev, R. V.; Georgiou, T.; Morozov, S. V.; Grigorenko, A. N.; Geim, A. K.; Casiraghi, C.; Castro Neto, A. H.; Novoselov, K. S. Strong Light-Matter Interactions in Heterostructures of Atomically Thin Films. *Science* **2013**, *340*, 1311.

(23) Butler, S. Z. Progress, Challenges, and Opportunities in Two-Dimensional Materials Beyond Graphene. *ACS Nano* **2013**, *7*, 2898−2926.

(24) Grigorenko, A. N.; Polini, M.; Novoselov, K. S. Graphene Plasmonics. *Nat. Photonics* **2012**, *6*, 749−758.

(25) Fei, Z.; Rodin, A. S.; Andreev, G. O.; Bao, W.; McLeod, A. S.; Wagner, M.; Zhang, L. M.; Zhao, Z.; Thiemens, M.; Dominguez, G.; Fogler, M. M.; Castro Neto, A. H.; Lau, C. N.; Keilmann, F.; Basov, D. N. Gate-Tuning of Graphene Plasmons Revealed by Infrared Nano-Imaging. *Nature* **2012**, *487*, 82.

(26) Chen, J.; Badioli, M.; Alonso-González, P.; Thongrattanasiri, S.; Huth, F.; Osmond, J.; Spasenović, M.; Centeno, A.; Pesquera, A.; Godignon, P.; Elorza, A. Z.; Camara, N.; de Abajo, F. J. G.; Hillenbrand, R.; Koppens, F. H. L. Optical Nano-Imaging of Gate-Tunable Graphene Plasmons. *Nature* **2012**, *487*, 77.

(27) Falkovsky, L. A. Optical Properties of Graphene. *J. Phys.: Conf. Ser.* **2008**, *129*, 012004.

(28) Jablan, M.; Buljan, H.; Soljačić, M. Plasmonics in Graphene at Infrared Frequencies. *Phys. Rev. B: Condens. Matter Mater. Phys.* **2009**, *80*, 245435.

(29) Christensen, J.; Manjavacas, A.; Thongrattanasiri, S.; Koppens, F. H. L; de Abajo, F. J. G. Graphene Plasmon Waveguiding and Hybridization in Individual and Paired Nanoribbons. *ACS Nano* **2012**, *6*, 431.

(30) Nikitin, A. Yu.; Guinea, F.; Garcia-Vidal, F. J.; Martin-Moreno, L. Edge and Waveguide Terahertz Surface Plasmon Modes in Graphene Microribbons. *Phys. Rev. B: Condens. Matter Mater. Phys.* **2011**, *84*, 161407.

(31) Dai, S.; Fei, Z.; Ma, Q.; Rodin, A. S.; Wagner, M.; McLeod, A. S.; Liu, M. K.; Gannett, W.; Regan, W.; Watanabe, K.; Taniguchi, T.; Thiemens, M.; Dominguez, G.; Castro Neto, A. H.; Zettl, A.; Keilmann, F.; Jarillo-Herrero, P.; Fogler, M. M.; Basov, D. N. Tunable Phonon Polaritons in Atomically Thin van der Waals Crystals of Boron Nitride. *Science* **2014**, *343*, 1125−1129.

(32) Xu, X. G.; Ghamsari, B. G.; Jiang, J. H.; Gilburd, L.; Andreev, G. O.; Zhi, C.; Bando, Y.; Golberg, D.; Berini, P.; Walker, G. C. One-Dimensional Surface Phonon Polaritons in Boron Nitride Nanotubes. *Nat. Commun.* **2014**, *5*, 4782.

(33) Afsar, M. N. Precision Millimeter-Wave Measurements of Complex Refractive Index, Complex Dielectric Permittivity, and Loss Tangent of Common Polymers. *IEEE Trans. Instrum. Meas.* **1987**, *IM-36*, 530−536.

(34) Riddle, B.; Baker-Jarvis, J.; Krupka, J. Complex Permittivity Measurements of Common Plastics Over Variable Temperatures. IEEE Trans. *IEEE Trans. Microwave Theory Tech.* **2003**, *51*, 727−733.

(35) http://www.rfcafe.com/references/electrical/dielectric-constants-strengths.htm.

DOI: 10.1021/acsphotonics.5b00503
ACS Photonics 2016, 3, 737−742

(36) Liu, M.; Yin, X.; Ulin-Avila, E.; Geng, B.; Zentgraf, T.; Ju, L.; Wang, F.; Zhang, X. A Graphene-Based Broadband Optical Modulator. *Nature* **2011**, *474*, 64−67.
(37) Li, W.; Chen, B.; Meng, C.; Fang, W.; Xiao, Y.; Li, X.; Hu, Z.; Xu, Y.; Tong, L.; Wang, H.; Liu, W.; Bao, J.; Shen, Y. R. Ultrafast All-Optical Graphene Modulator. *Nano Lett.* **2014**, *14*, 955−959.
(38) Chen, B. G.; Meng, C.; Yang, Z.; Li, W.; Lin, S.; Gu, Y.; Guo, X.; Wang, D.; Yu, S.; Wong, C. W.; Tong, L. Graphene Coated ZnO Nanowire Optical Waveguides. *Opt. Express* **2014**, *22*, 24276−24285.
(39) Slepyan, G. Ya.; Maksimenko, S. A.; Lakhtakia, A.; Yevtushenko, O.; Gusakov, A. V. Electrodynamics of Carbon Nanotubes: Dynamic Conductivity, Impedance Boundary Conditions, and Surface Wave Propagation. *Phys. Rev. B: Condens. Matter Mater. Phys.* **1999**, *60*, 17136.
(40) Zhang, Q.; Hároz, E. H.; Jin, Z.; Ren, L.; Wang, X.; Arvidson, R. S.; Lüttge, A.; Kono, J. Plasmonic Nature of the Terahertz Conductivity Peak in Single-Wall Carbon Nanotubes. *Nano Lett.* **2013**, *13*, 5991−5996.
(41) Prade, B.; Vinet, J. Y. Guided Optical Waves in Fibers With Negative Dielectric Constant. *J. Lightwave Technol.* **1994**, *12*, 6−18.
(42) Schroter, U.; Dereux, A. Surface Plasmon Polaritons on Metal Cylinders With Dielectric Core. *Phys. Rev. B: Condens. Matter Mater. Phys.* **2001**, *64*, 125420.
(43) Catrysse, P. B.; Fan, S. Understanding the dispersion of coaxial plasmonic structures through a connection with the planar metal-insulator-metal geometry. *Appl. Phys. Lett.* **2009**, *94*, 231111.
(44) Krasavin, A. V.; Zayats, A. V. Silicon-Based Plasmonic Waveguides. *Opt. Express* **2010**, *18*, 11791.
(45) Brar, V. W.; Jang, M. S.; Sherrott, M.; Kim, S.; Lopez, J. J.; Kim, L. B.; Mansoo, C.; Atwater, H. Hybrid Surface-Phonon-Plasmon Polariton Modes in graphene/Monolayer h-BN Heterostructures. *Nano Lett.* **2014**, *14*, 3876−3880.
(46) Okamoto, K. *Fundamentals of Optical Waveguides*,2nd ed.; Academic Press, 2005.
(47) Ebendorff-Heidepriem, H.; Foo, T. C.; Moore, R. C.; Zhang, W.; Li, Y.; Monro, T. M.; Hemming, A.; Lancaster, D. G. Fluoride Glass Microstructured Optical Fiber with Large Mode Area and Mid-Infrared Transmission. *Opt. Lett.* **2008**, *33*, 2861−2863.

DOI: 10.1021/acsphotonics.5b00503
ACS Photonics 2016, 3, 737−742